6-2022

Oligomerization of amyloid-β peptide in the presence of gangliosides–Implications for Alzheimer disease

Sydney Boyd
The University of Southern Mississippi

Oligomerization of amyloid-β peptide in the presence of gangliosides – Implications for Alzheimer disease

by

Sydney Boyd

A Thesis
Submitted to the Honors College of
The University of Southern Mississippi
in Partial Fulfillment
of Honors Requirements

May 2022

Approved by:

Vijay Rangachari, Ph.D., Thesis Advisor,
School of Mathematics and Natural Sciences

Bernd Schroeder, Ph.D., Director,
School of Mathematics and Natural Sciences

Sabine Heinhorst, Ph.D., Dean
Honors College

ABSTRACT

Alzheimer disease (AD) is a neurodegenerative disorder that leads to memory impairment and cognitive dysfunction in elderly populations worldwide. A key characteristic of AD is the formation of neuritic plaques composed of extracellularly deposited aggregates of amyloid-β (Aβ), an intrinsically disordered protein. Although Aβ fibrils were once thought to be the prime initiators of the disease, research has since been shifted to consider soluble, low molecular weight Aβ oligomers as the driving force behind AD toxicity. Due to its origin as a cleavage product of amyloid precursor protein (APP), an integral membrane protein, Aβ is known to perpetually interact with a variety of membrane lipids. We have previously characterized oligomerization of Aβ42 with lipid and fatty acids as well as GM1 ganglioside, an abundant component of membrane lipid rafts. These oligomers, coined GM1Os, exhibit unique biochemical and biophysical properties. Additionally, low levels of neurotransmitters such as acetylcholine (ACh) and dihydroxyphenylacetaldehyde (DOPAL) have been implicated in the onset of AD. This project involves the characterization of GM3- and GD3- bound Aβ42, which exhibits distinct properties, conformation, and effects on Aβ aggregation. Similarly, ACh and DOPAL were found to inhibit the aggregation of Aβ, confirming correlation between low levels of neurotransmitters and plaque formation. These findings suggest that different neuronal gangliosides interact differently with Aβ, which has implications on the varying degrees of toxicity in clinical AD pathology.

Keywords: *amyloid-beta, protein aggregation, Alzheimer diseas, Oligomers, lipids*

ACKNOWLEDGMENTS

I joined Dr. Rangachari's lab in January of 2020, and the amount of gratitude I have felt in the last two years could fill another document entirely. My first thanks is to Dr. Rangachari, for his willingness to allow me to join his lab so early in my undergraduate career and for his constant guidance throughout the duration of my research. Not only did his support lead me to complete this project, but it also opened the door for other accomplisments and acheivements over the course of his mentorship.

Of course, I could never have completed this thesis without the guidance of my graduate student mentor and friend Jhinuk Saha. The amount of time, effort, and care she put into teaching and helping me succeed is immense, and I cannot possibly express the amount of gratitude I have for her.

Finally, I would like to thank both the Drapeau Center at The Univeristy of Southern Mississippi for awarding me Eagle SPUR funding and the Honors College for constantly challenging me to reach my full potential as a scholar

TABLE OF CONTENTS

LIST OF ILLUSTRATIONS

Deleted:

LIST OF ABBREVIATIONS

AD	Alzheimer disease
Aβ	amyloid-β
CAA	cerebral amyloid angiopathy
APP	amyloid precursor protein
ADDL	Aβ-derived diffusible ligand
CAT	choline acetyltransferase
ACh	acetylcholine
DOPAL	dihydroxyphenylacetaldehyde
DOPAL-SO	DOPAL-derived αS oligomer
NEFA	non-esterified fatty acid
LFAO	large fatty acid-derived oligomer
GM1O	GM1-dervied oligomer
LPG	lysophosphatidyl glycerol
SEC	size exclusion chromatography
MALDI-Tof	matrix-assisted laser desorption time-of-flight
ThT	thioflavin-T
SDS PAGE	sodium dodecyl sulfate-polyacrylamide gel electrophoresis
PK	proteinase K

CHAPTER I: INTRODUCTION

1.1 Alzheimer disease

Alzheimer disease (AD) is a neurodegenerative disease that affects approximately 44 million people internationally, a figure that is projected to nearly double by 2030[1]. Characterized by progressive loss of cognitive function and memory among elderly patients, AD has increasingly become an issue for medical systems to navigate as the average life expectancy increases[2]. There are two major types of lesions involved in neuronal dysfunction and toxicity: intracellular neurofibrillary tangles and extracellular neuritic plaques. The neurofibrillary tangles, composed of hyper-phosphorylated tau proteins, lead to neuronal death [3]. The neuritic plaques are deposits of Amyloid-β (Aβ) peptide aggregates that abundantly assemble in the limbic systems of AD-afflicted brains, causing damage to neurons in plaque vicinity[2].

1.2 Aβ

Following the isolation of Aβ peptide from both cerebral amyloid angiopathy (CAA) amyloid deposits and AD neuritic plaques from post mortem brains in the 1980s, the mechanisms behind the generation of Aβ and its plaques have been vastly studied[4–6]. Aβ is produced upon proteolytic cleavage of amyloid precursor protein (APP), a type I integral membrane protein located within the central nervous system with a localized isoform consisting of 695 amino acids[7]. Under conditions that remain unclear, APP can be cleaved by α-secretase to generate soluble protein fragments; this process is called the non-amyloidogenic pathway. Aβ, however, is produced in the amyloidogenic pathway, in which APP is sequentially cleaved into fragments by β-secretase and γ-secretase[8]. The

Aβ monomers produced by this cleavage are intrinsically disordered and its isoforms can have 39 to 43 amino acid residues, with Aβ40 and Aβ42 isoforms being the main components in neuritic plaques[6,8,9].

In the early 1990s, Hardy and Higgins proposed the amyloid cascade hypothesis, suggesting that deposits of Aβ fibrils were the main contributors to the onset of AD symptoms, triggering neurofibrillary tangle formation and neuronal death in response[9]. Revisions to the amyloid cascade hypothesis were prompted upon the discovery of Aβ-derived diffusible ligands (ADDLs), soluble Aβ oligomers that were neurotoxic in organotypic mouse brain slice cultures in the absence of insoluble fibrils[10]. This discovery, corroborated with significant indication that amyloid plaque formation could not be directly linked to synapse loss or cognitive decline in AD-afflicted brains, has shifted research focus on the propagation of these soluble Aβ oligomers, which are hypothesized to initiate toxic pathways much earlier than the formation of plaques[11,12]. Much evidence has since been reported that interactions of Aβ with proteins involved in other neurodegenerative diseases, metal-ions, and various other metabolites uniquely influence aggregation kinetics, oligomerization, and AD pathology compared to homotypic Aβ fibrillar formation[13–15].

1.3 Possible effects of neurotransmitters on Aβ aggregation

Following the proteolytic cleavage of APP, Aβ is formed in the extracellular space and is consequentially prone to interact with a variety of neurotransmitters, which are abundant in the synaptic cleft. Since studies first indicated drastically decreased levels of choline acetyltransferase (CAT) in AD brain biopsies, it has been documented that low

levels of neurotransmitter acetylcholine (ACh) are likewise corroborated with the disease[16–18]. In the basal forebrains of AD-afflicted brains, neurons responsible for the release of ACh degenerate selectively during the onset of the disease. We have also established that the protein α-synuclein (αS), the primary causative agent of Parkinson's disease, interacts with dopamine metabolite dihydroxyphenylacetaldehyde (DOPAL) to form unique oligomers called DOPAL-derived αS oligomers (DOPAL-SOs). The cross-seeding of Aβ42 with these DOPAL-SOs formed conformationally distinct fibrils[19]. Despite the significant evidence that AD pathology is linked to neurotransmitters like ACh and DOPAL, the mechanism and effect of their interaction with Aβ is still poorly understood. A key step in understanding the role of neurotransmitters in neuritic plaque formation is to characterize neurotransmitter-Aβ oligomers with distinct conformations and biophysical properties.

1.4 Aβ-lipid interactions

Inherent to its origin from the transmembrane protein APP and its amphipathic nature, Aβ has a strong affinity toward membrane phospholipids to generate aggregates with varying levels of cytotoxicity[20–23]. However, the formation of lipid-induced fibrils is contingent upon various conditions *in vitro*. For instance, anionic phospholipids have been shown to increase Aβ fibrillar formation, but only when certain structural moieties, including fatty acids, phosphate groups, and C-terminal aliphatic amino acids, are present[24]. It has also been shown that lipids differentially influence the mechanism of fibrillar formation, including the rate of aggregation of monomeric Aβ versus oligomeric Aβ, as well as mutant Aβ[25–28].

Furthering the endeavor to understand Aβ-lipid interactions, our lab has characterized multiple distinct oligomer conformations in the presence of lipids. For example, it was determined that conformationally distinct low-molecular weight Aβ oligomers result from propagation with non-esterified fatty acids (NEFAs), which are copious within the brain[29]. Shortly after, these oligomers, coined large fatty acid-derived oligomers (LFAOs), were found to initiate the conversion of Aβ42 monomers into LFAOs[30]. This work was corroborated with the characterization of LFAO-seeded fibrils, which presented distinct conformations opposed to homotypic Aβ fibrils[31].

Ganglioside interactions with Aβ have also been a focal point in understanding the influence of lipids on Aβ aggregation. Following the characterization of a novel GM1 ganglioside-bound Aβ species by Yanagisawa et al., it was been established that GM1, a chief constituent of lipid rafts found abundantly in neurons, instigates a β-sheet transition state in Aβ monomer[32,33]. Similar to LFAOs, GM1-bound Aβ has also been shown to seed the fibrillation of monomeric Aβ in membranes mimicking the lipid composition of rafts[34]. Recent data from our lab established that GM1-dervied oligomers (GM1Os) exhibit unique conformations, biophysical characteristics, and cytotoxicity to a greater extent than anionic lysophosphatidyl glycerols (LPGs), which were biophysically similar to LFAOs[35].

Interestingly, it has been suggested that the location of Aβ plaque distribution in the brain is moderated by different gangliosides. Yamamoto et al. reported that the aggregation of hereditary Aβ variants in different regions of the brain is influenced by the type of ganglioside abundant in such region. For instance, GM3 ganglioside positively influenced the aggregation of Dutch- and Italian-type Aβ variants, while GD3 ganglioside

enhanced aggregation of the Flemish-type Aβ variant. This suggests that the localization of Aβ to a particular region of the brain is ganglioside-dependent[36].

1.5 Focus of this research

Motivated by the lack of understanding surrounding the pathology of Aβ oligomers in AD, we aim to characterize Aβ oligomers generated from both neurotransmitter interactions and with ganglioside-enriched lipids to investigate their biophysical properties. Such an investigation would lead to discoveries on oligomer strain generation with distinct conformations implicated in various phenotypes observed in patient brains.

CHAPTER II: MATERIALS AND METHODS

2.1 Materials

The C8 Zorbax semi-prep HPLC column was purchased from Agilent. The size exclusion chromatography (SEC) column (Superdex-75 HR 10/30) used to purify monomers was bought from GE Life Sciences (Marlborough, MA). Ab5 monoclonal antibody was obtained from the laboratory of Dr. Levites (University of Florida, Gainesville). Acetylcholine (ACh) was purchased from Sigma-Aldrich, while DOPAL was purchased from Cayman Chemicals (Ann Arbor, Michigan). Lipid stocks (GM1 and GM3) were procured from Avanti Polar Lipids, Inc (Alabaster, AL).

2.2 Preparation of Aβ monomers

Wild type Aβ42 plasmid obtained from Addgene was used to transform *Escherichia coli* BL21 (DE3) cells, which were then grown in LB broth containing ampicillin to an optical density (OD) of 0.7 at 600 nm and induced with 1 mM IPTG for 16-18h at 37º C. Cells were harvested at 9500 xg for 15 minutes and cell pellets were stored at -20° C. For Aβ purification, cells were resuspended in TE buffer (20 mM Tris, pH 8.0, 1 mM EDTA and subjected to 10 sonication cycles (30 second burst, 1 minute rest). Sonicated cells were centrifuged at 9500 xg for 15 minutes and the pellet was again resuspended in TE buffer and sonicated for 8 cycles (30 second burst, 1 minute rest), before being centrifuged at 9500 xg for 15 minutes. The pellet was again resuspended in buffer for 6 sonication cycles (30 second burst, 1 minute rest). The resulting pellet containing the inclusion bodies was then resuspended in TE buffer containing 4 M Urea and sonicated for 6 cycles. The supernatant collected from centrifugation was filtered

through a hydrophilic PVDF membrane (Millipore Sigma) into 1 mL aliquots into siliconized Eppendorf tubes and stored at -80º C until needed for HPLC purification.

1 mL aliquots of Aβ were loaded onto a C8 Zorbax semi-prep HPLC column that had been preheated for 45 minutes in an 80º C water bath. The column was attached to an HPLC system that had been preheated to 66.5ºC, and reversed phase HPLC was completed with a starting gradient of 95% (v/v) H_2O and 5% (v/v) acetonitrile and a flow rate of 1.5 mL/min. Samples were collected in 1 mL fractions. A Cary 50-UV-vis spectrometer (Agilent Technologies, Inc; Santa Clara, CA) was used to determine concentration of Aβ in collected fractions, and samples were lyophilized before storing at -80º C for subsequent SEC chromatography purification of Aβ monomers.

Before loading onto the SEC column (Superdex-75 HR 10/30), lyophilized Aβ peptide stored at -80º C was dissolved in nanopure H_2O (490µL) for 30 minutes at room temperature and NaOH (10 mM) for 10 minutes. The Superdex-75 HR 10/30 SEC column was then connected to a BioLogic DuoFlowTM chromatography system, and Aβ in NaOH was ran in 20 mM Tris buffer (pH 8.0) at a rate of 0.5 mL/min at 25º C. The purified monomers were collected and the appropriate monomer fractions were pooled. The Aβ concentration was determined with a Cary 50-UV-vis spectrophotometer, using a molar extinction coefficient of 1450 M^{-1} cm^{-1} at 276 nm. To validate the purity of the Aβ monomers, matrix-assisted laser desorption time-of-flight mass spectrometry (MALDI-Tof) was performed. Purified monomers were stored in siliconized Eppendorf tubes at 4º C and used within 5-6 hours.

2.3 Thioflavin-T fluorescence

Aggregation kinetics of Aβ and its reaction with other biomolecules were monitored by thioflavin-T (ThT) fluorescence for 48 hours at 37º C in a BioTek Synergy 96 well plate reader. Neurotransmitter reactions were carried out with Aβ monomer (25 μM) with various concentration of acetylcholine (0.1, 10, and 50 mM) and DOPAL (0.1, 0.5, 1.75, 2.5, 3.5 mM) in the presence of 50 μM ThT in 20mM Tris buffer (pH-8.0). Ganglioside reactions were carried out similarly, with Aβ monomers (25 μM) in 20 mM Tris (pH 8.0), 50 mM NaCl, and 50 μM ThT, with 75 μM GM1, 400 μM GM3, 100 μM GD3, and 400 μM GD3 micelles, respectively. Each reaction was transferred in 200 μL aliquots to a Corning 96-well plate (black plates) for aggregation kinetics. Samples were excited at 452 nm, and ThT fluorescence was obtained with an emission at 485 nm at every 10 minutes at 37ºC with shaking.

2.4 Gel electrophoresis and immunoblotting

Prior to sodium dodecyl sulfate-polyacrylamide gel electrophoresis (SDS-PAGE), 1X Laemmli loading buffer containing 1% (w/v) SDS was added to samples before loading onto a 4%-20% (w/v) Bis-Tris Bio-Rad TGX gel without heating. For fragment molecular weight comparison, pre-stained molecular weight markers (Novex Sharp Protein Standard, Life Technologies) were ran in parallel. Following PAGE denaturation, gels were immunoblotted onto a 0.2 μM nitrocellulose membrane (Bio-Rad) and boiled in 1X PBS (pH 7.4) in a microwave oven for 1 minute. The immunoblot was then blocked in 1X PBS (pH 7.4) containing 5% (w/v) nonfat dry milk and 1% (v/v) Tween-20 for 1.5 hours at 25º C, before being probed overnight with Aβ-specific Ab5

monoclonal antibody (1:6000 dilution) at 4º C. An anti-mouse, horseradish peroxidase-conjugated secondary antibody (1:6000 dilution) was then used to probe the immunoblot for 1.5 hours at 25º C. Blots were then imaged using a GelDoc molecular imager (Bio-Rad) and a Super SignalTM West Pico Chemiluminescent Substrate kit (Thermo Fisher Scientific).

2.5 Digestion with Proteinase K (PK)

PK digestion was carried out by mixing 5 μM samples of Aβ-GM1 and Aβ-GM3 samples and 2 nM PK diluted from 20 mg/mL stock solution (Ambion Corporation) to a 10 nM stock in 20 mM Tris (pH 8.0) and incubating the reactions at 37º C while shaking at 200 rpm. Reactions were then quenched with 0.5 mM PMSF at time intervals of 10, 20, 30, and 40 minutes. SDS PAGE was then carried using 1% (w/v) SDS-PAGE and immunoblotted with Ab5 monoclonal antibody for imaging.

CHAPTER III: RESULTS

3.1 Neurotransmitters ACh and DOPAL inhibit Aβ42 aggregation

The effect of neurotransmitters ACh and DOPAL on Aβ42 aggregation kinetics were monitored by ThT binding at 37º C for 24 hours. In these assays, we saw that increasing concentrations of ACh induced an increase in the lag times of Aβ42 aggregation (Fig. 1A). The lowest stoichiometry of ACh (100 µM) showed a lag time of

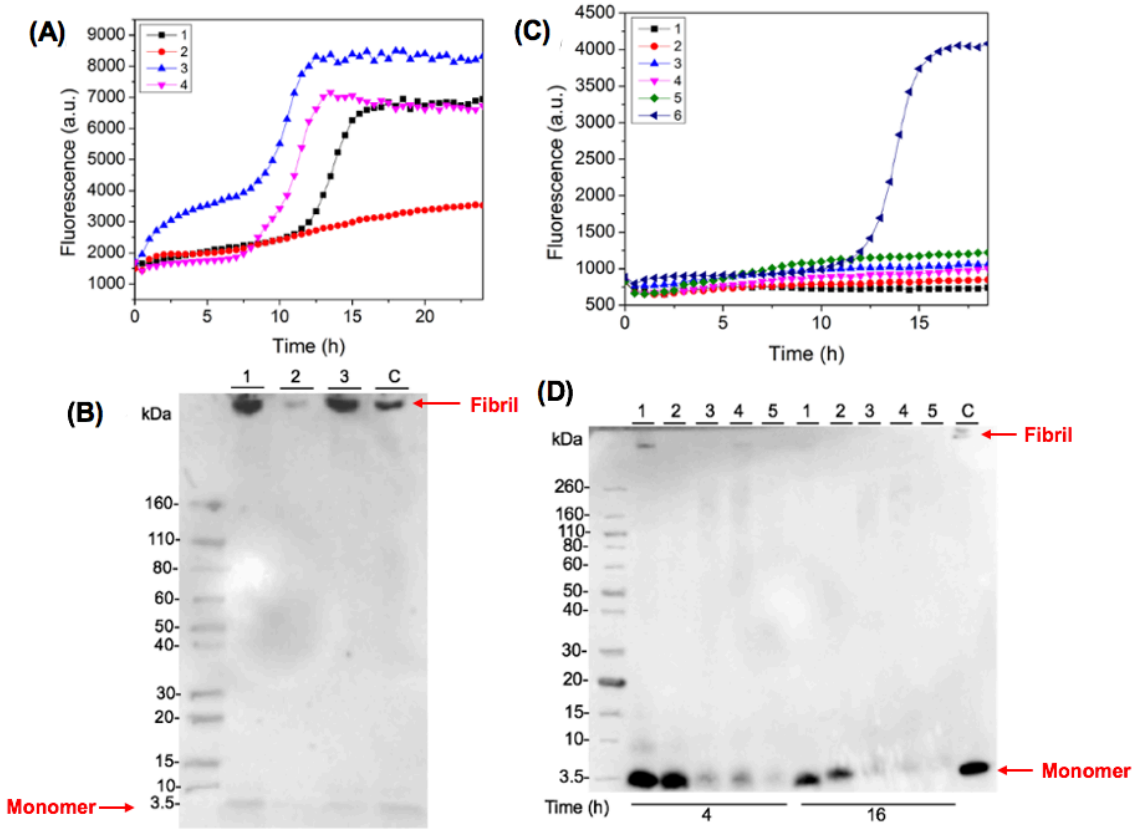

Figure 1: ThT fluorescence of Aβ interactions with neurotransmitters. (A) Aggregation kinetics of 10 µM Aβ in 20 mM Tris Buffer (pH 8.0) and 50 µM ThT with 10 mM ACh (1, black squares), 50 mM ACh (2, red circles), 100 µM ACh (3, blue triangles), and Aβ control alone (4, magenta triangles). **(B)** Aggregation kinetics of 10 µM Aβ in 20 mM Tris Buffer (pH 8.0) and 50 µM ThT with 100 µM DOPAL (1, black squares), 500 µM DOPAL (2, red circles), 1.75 mM DOPAL (3, blue triangles), 2.50 mM DOPAL (4, magenta triangles), 3.50 mM DOPAL (5, green diamonds), and Aβ control (6, navy triangles). **(C)** Western blot following SDS-PAGE of the incubation of 10 µM Aβ in 20 mM Tris Buffer (pH 8.0) with 10 mM ACh (1), 50 mM ACh (2), 100 µM ACh (3), and Aβ control (C). **(D)** Western blot following SDS-PAGE of the incubation of 10 µM Aβ in 20 mM Tris Buffer (pH 8.0) with 100 µM DOPAL (1), 500 µM DOPAL (2), 1.75 mM DOPAL (3), 2.50 mM DOPAL (4), 3.50 mM DOPAL (5), and Aβ control (C) at 4 and 16 hours, respectively.

7-8 hours, close to the control of Aβ42 alone, indicating that in our experimental setup, 100 μM of Ach had no effect on the aggregation rate of Aβ42. At the higher concentrations of ACh, however, lag times of Aβ42 aggregation increased, with 10 mM ACh inducing aggregates at 11-12 hours and 50 mM ACh inducing aggregates at 24 hours (Fig. 1A). This suggests that higher concentrations of ACh inhibit Aβ42 aggregation. Following incubation of the same reactions at 37º C for 24 hours, SDS-PAGE confirmed that 50 mM ACh inhibited Aβ42 aggregation, as indicated by the diminished intensity of molecular weight band in the fibril region as opposed to the control (Fig. 1B). Figure 1C shows ThT fluorescence analysis of the DOPAL induced Aβ42 aggregates. At each concentration of DOPAL, the lag time of Aβ42 was significantly increased, suggesting that each tested concentration of DOPAL inhibited Aβ42 aggregation. A parallel analysis of these samples by SDS-PAGE and Western Blot showed the control Aβ42 in the absence of neurotransmitters formed a high molecular weight band that failed to enter the gel, indicating fibril formation (Fig. 1D, Lane C). In contrast, samples incubated with DOPAL showed no such bands but a prominent monomeric band near 4.5 kDa, suggesting that DOPAL effectively inhibited aggregation correlating to the ThT data (Fig. 1D, Lanes 2-5, 4 hours; Lanes 1-5, 16 hours).

3.2 The effect of GM3 and GD3 ganglioside micelles on Aβ42 aggregation.

Previous data in our laboratory indicated that lipid surface characteristics can alter the course Aβ aggregation to generate unique oligomers[35]. To see whether differences in carbohydrate distributions on gangliosides have a similar effect on Aβ aggregation, GM3, GD3 and GM1 ganglioside micelles were incubated with Aβ42 and aggregation was

monitored (Fig. 2A). Our analysis showed that each concentration of ganglioside micelles induced aggregation of Aβ42 before the lag time of the control, suggesting that all gangliosides tested increased the rate of Aβ42 aggregation (Fig. 2A).

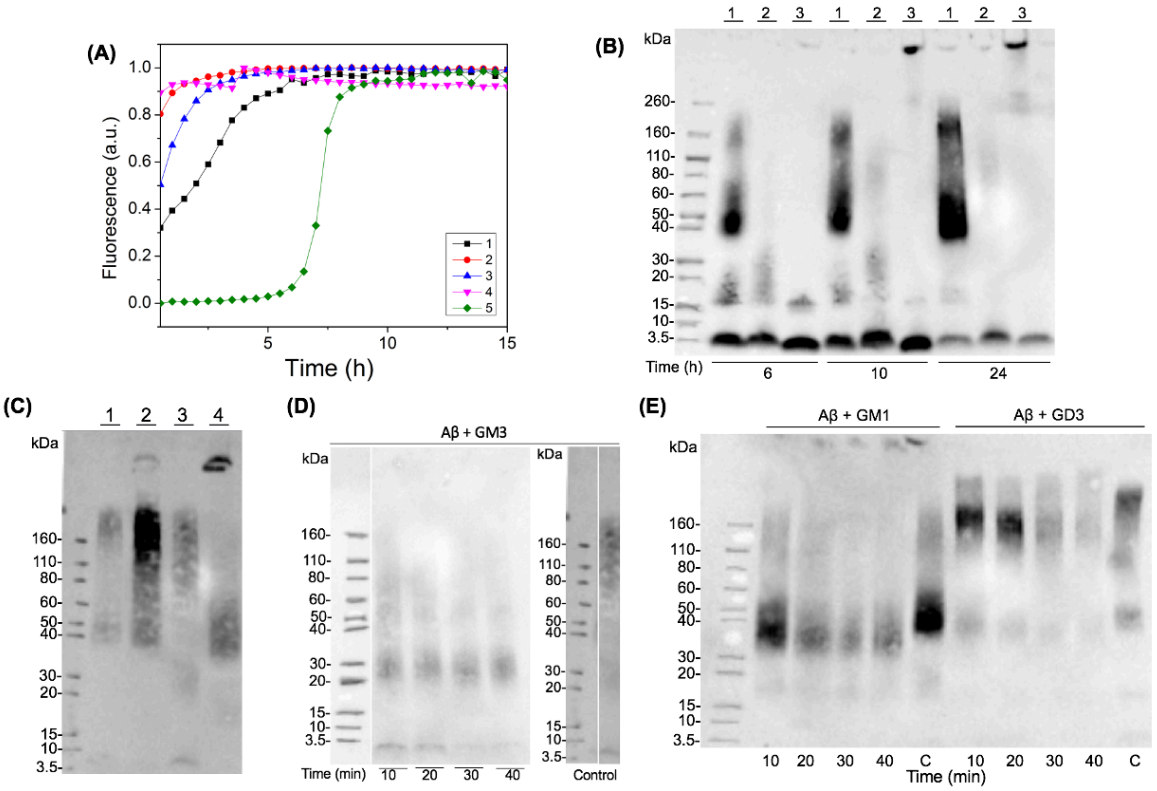

Figure 2: Interactions of gangliosides GM3 and GD3 with Aβ. (A) ThT fluorescence of 25 μM Aβ with 75 μM GM1 (1, black squares), 400 μM GM3 (2, red circles), 400 μM GD3 (3, blue triangles), 100 μM GD3 (4, magenta triangles), and Aβ control (5, green diamonds) in 20 mM Tris (pH 8.0), 50 mM NaCl, and 50 μM ThT **(B)** Incubation of 25 μM Aβ with 75 μM GM1 (1), 400 μM GM3 (2), and Aβ control (3) in 20 mM Tris (pH 8.0) and 50 mM NaCl at time frames of 6 hours, 10 hours, and 24 hours. **(C)** Incubation of 25 μM Aβ with 400 μM GD3 (1), 100 μM GD3 (2), 400 μM GM3 (3), and 75 μM GM1 (4) in 20 mM Tris (pH 8.0) and 50 mM NaCl. **(D)** Proteinase K digestion of 25 μM Aβ and 400 μM GM3 for time intervals of 10, 20, 30, and 40 minutes with Aβ control to the right. **(E)** Proteinase K digestion of 25 μM Aβ with 75 μM GM1 and 100 μM GD3 for time intervals of 10, 20, 30, and 40 minutes. Aβ control labeled C.

After incubation of with GM3, Aβ formed high molecular weight (HMW) aggregates after 10-24 hours (Fig. 2B), along with fibrils. Upon centrifugation and isolation by SEC, the presence of the HMW aggregate band diminished, indicating that Aβ did not form a stable oligomer (Fig. 3A). Incubation of Aβ with GD3 likewise formed HMW aggregates after 24 hours (Fig. 2C), along with fibrils. However, soluble oligomers

were able to be separated using centrifugation and isolation by SEC. The isolated aggregates of Aβ-GD3 did appear to be stable and oligomeric (Fig. 3B).

Proteinase K (PK) digestion is commonly used to assess enzymatic stabilities of aggregates, which also reflects the conformational differences and similarities among aggregates[37–39]. Therefore, PK was used to determine conformational differences and stability of the oligomers formed in the presence of GM3- and GD3-induced Aβ42 aggregates. Figure 2D displays the Western Blot of PK digestion with 400 μM GM3-induced Aβ aggregates at time intervals of 10, 20, 30, and 40 minutes. The HMW oligomer band begins to diminish after 10 minutes of digestion; however, GD3-Aβ42 aggregates seem to withstand PK digestion throughout each digestion time (Fig. 2E). As seen by the diminishing oligomeric band at 30 and 40 minutes, GD3-Aβ42 aggregates withstood digestion to a lesser extent than the established GM1-induced Aβ oligomer (Fig. 2E).

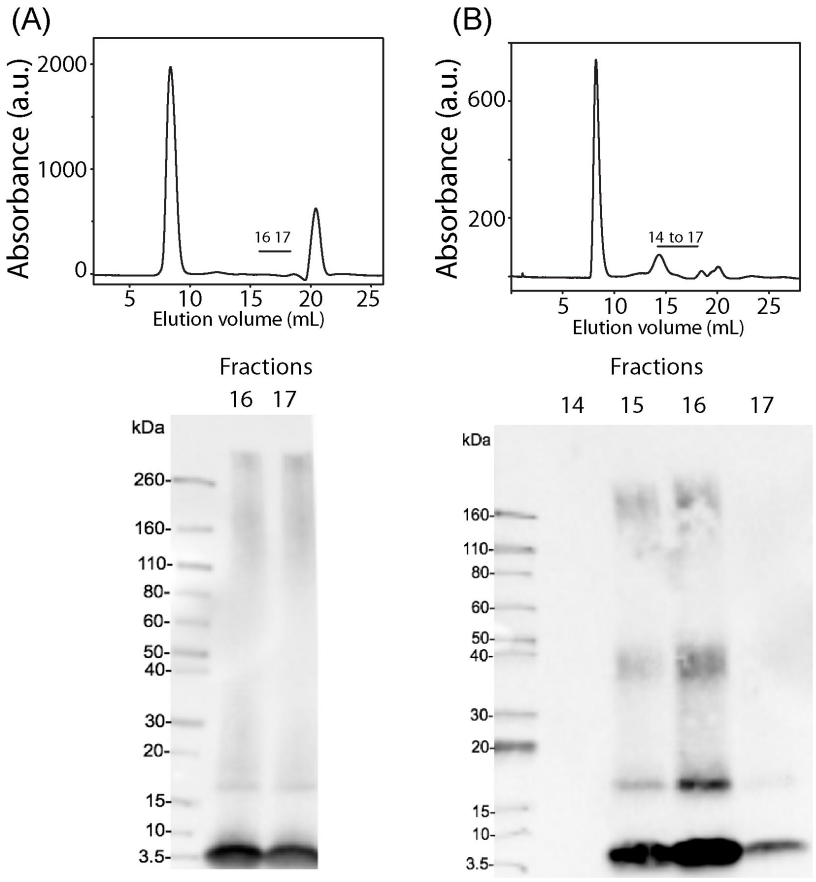

Figure 3: SDS-PAGE of Aβ aggregates isolated by SEC. (A) GM3-induced Aβ aggregates and **(B)** GD3-induced Aβ aggregates. SEC fractions are labeled accordingly.

These results suggest that Aβ-GM3 and Aβ-GD3 are digested differently than the established Aβ-GM1 oligomer, and in turn establish that these oligomers have possible conformational differences.

3.3 Expression and purification of recombinant AβE22Δ (Osaka) mutant

Aβ with a deletion mutation at amino acid position 22 are refered to as the Osaka variant (AβE22Δ), which has been shown to increase the rate of oligomer formation, causing symptoms of AD to appear earlier than the typical patient age range[40]. We sought to determine the effects of this mutant in the presence of the ganglioside lipids not only to uncover the significance of the glutamate residue in oligomer formation but also to provide support for the potential role of gangliosides in pathogenesis with Osaka variant.

We therefore designed experiments to determine the effects of GM1, GM3 and GD3 on Aβ Osaka oligomerization. Osaka Aβ42 was subcloned into a plasmid at the Florida State University Cloning Facility and subsequently used to transform competent *Escherichia coli* BL21 (DE3) cells. Cultures were checked for expression via dot blot

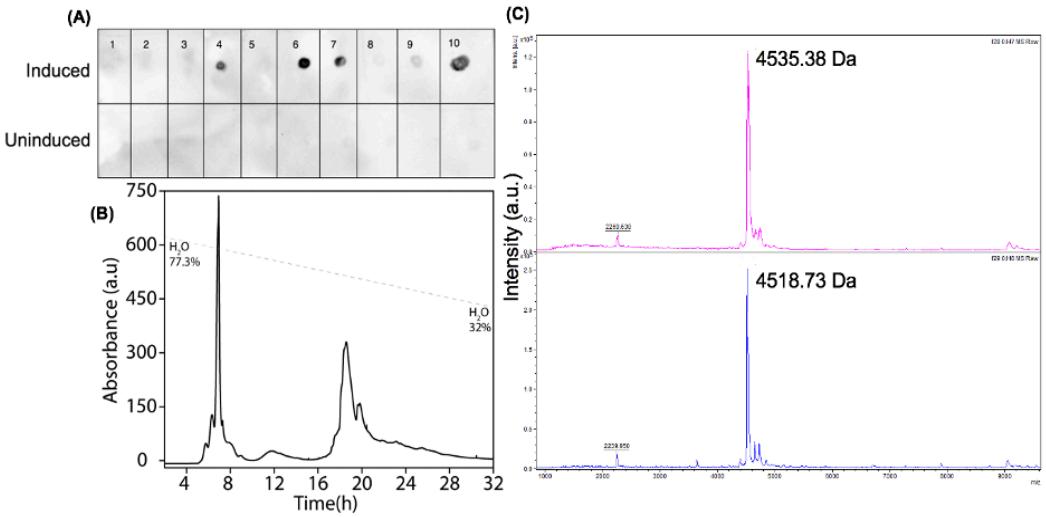

Figure 4: Recombinant Aβ Osaka variant transformation and purification. (A) Aβ Osaka expression check dot blot. (**B)** HPLC purification of recombinant Aβ Osaka. **(C)** Mass spectrometry analysis of HPLC-purified Aβ Osaka.

(Figure 4A), and colony 10 was selected for purification. Purification of recombinant Aβ Osaka colony 10 was conducted in the standardized recombinant wildtype Aβ42 purification and extraction method outlined in the Methods section. HPLC analysis showed that the peak typical of WT Aβ42 at 18 minutes was present (Figure 4B), indicating that recombinant Aβ Osaka purification was successful. MADLI-TOF mass spectrometry confirmed that the obtained protein was purified recombinant Aβ Osaka (theoretical mass: 4513 Da).

CHAPTER IV: DISCUSSION

The results presented here are aimed at increasing our understanding of Aβ oligomerization and thus their role in AD pathogenesis. Studies over the last decade have revealed the relevance of the oligomeric forms of Aβ to toxicity in AD, warranting studies focusing on factors that affect their formation[13-15]. Also, structural differences in the oligomeric forms of the protein have been shown to give rise to different pathological phenotypes in AD[19,35]. Accordingly, we investigated the oligomerization of Aβ in the presence of gangliosides and neurotransmitters and characterized their conformational differences. Here, we have shown data that suggests that differences in ganglioside structures contribute to these differential pathways in Aβ aggregation.

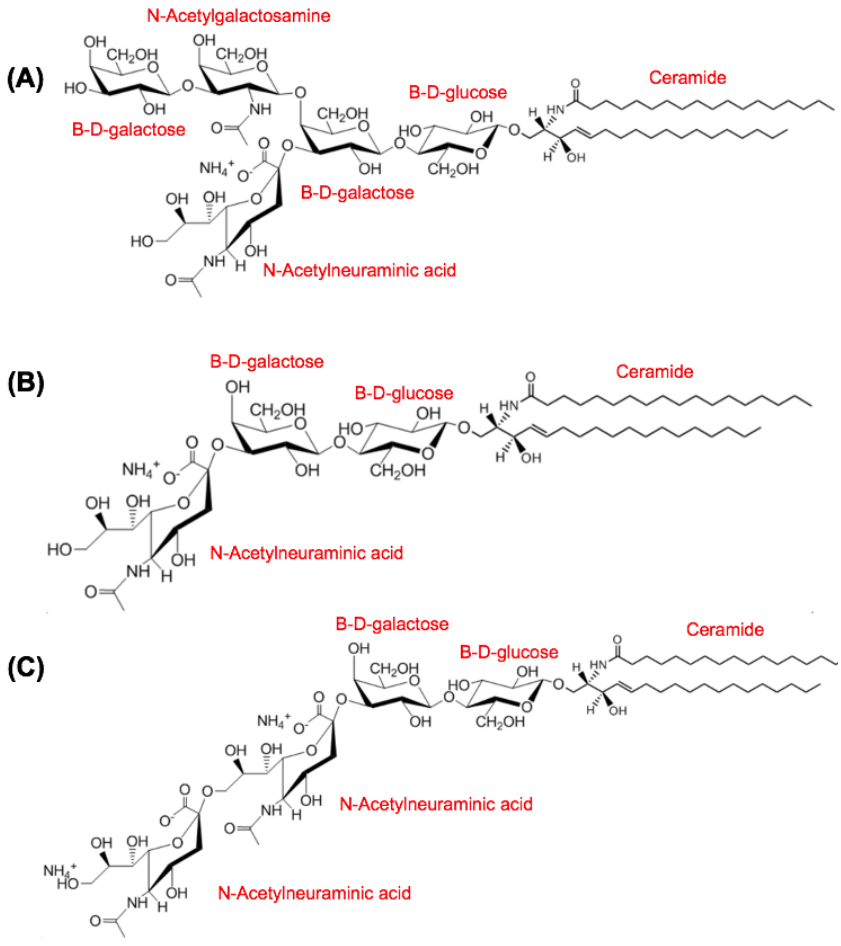

Figure 5: Structure of gangliosides GM1 (A), GM3 (B), and GD3 (C).

All gangliosides share a common ceramide attached to the lipid tail and a sialic acid connected to its carhbohydrate chain, but have distinction in their carbohydrate moieties (Fig. 5). Our results suggest that these chemical differences may manifest to differences in their interactions with Aβ (Fig. 2, Fig. 3). With all gangliosides tested here (including GM1, GM3, and GD3), the rate of Aβ42 aggregation was increased over controls (Fig. 2A). As compared to the stable, isolated GM1O established in the Rangachari lab [35], GM3- and GD3- induced oligomers also exhibit conformational differences with regard to their stability in the presence of PK (Fig. 2D, Fig. 2E). GD3-bound Aβ42 forms a more stable oligomer upon isolation and withstands PK digestion to a greater extent than GM3-bound Aβ42. Despite this finding, neither the GD3-bound Aβ42 or GM3-bound Aβ42 formed oligomers as stable as the established GM1O[35]. Differences in ganglioside composition is seen in various anatomical regions of the brain[36,41]. Our results are well aligned with the hypothesis that membrane constituents and surface characteristics contribute to the formation of different aggregation pathways and conformationally distinct oligomers[32–35].

The precise effect of neurotransmitters on the aggregation of Aβ has not been fully established. We believed that, alongside gangliosides, neurotransmitters modulate the aggregation and oligomerization of Aβ. My results on the effect of neurotransmitters on Aβ42 aggregation suggest that high concentrations of ACh and all tested concentrations of DOPAL inhibit the rate of aggregation. These findings, paired with the known loss of cholingeric neurons in AD pathology, suggest that possible remedies to the disease might involve endeavors to reintroduce these neurotransmitters to the synaptic cleft[16-18].

Overall, these results represent a preliminary step in understanding how the complex biochemistry of the neuronal environment affects the aggregation of Aβ. Here, we have established the potential role of neuronal gangliosides and neurotransmitters as modulators of Aβ aggregation, suggesting their use as therapeutic targets.

REFERENCES

1. International, A. D., Albanese, E., Guerchet, M., Prince, M. & Prina, M. World Alzheimer Report 2014: Dementia and risk reduction: An analysis of protective and modifiable risk factors. (2014).
2. Selkoe, D. J. Alzheimer's disease: genes, proteins, and therapy. *Physiol*. *Rev*. **81**, 741–766 (2001).
3. de Paula, V. de J. R., Guimarães, F. M., Diniz, B. S. & Forlenza, O. V. Neurobiological pathways to Alzheimer's disease: Amyloid-beta, TAU protein or both? *Dement*. *e Neuropsychol*. **3**, 188–194 (2009).
4. Glenner, G. G. & Wong, C. W. Alzheimer's disease: initial report of the purification and characterization of a novel cerebrovascular amyloid protein. *Biochem*. *Biophys*. *Res*. *Commun*. **120**, 885–890 (1984).
5. Masters, C. L. *et al*. Amyloid plaque core protein in Alzheimer disease and Down syndrome. *Proc*. *Natl*. *Acad*. *Sci*. *U*. *S*. *A*. **82**, 4245–4249 (1985).
6. Younkin, S. G. The role of Aβ42 in Alzheimer's disease. *J*. *Physiol*. **92**, 289–292 (1998).
7. O'Brien, R. J. & Wong, P. C. Amyloid Precursor Protein Processing and Alzheimer's Disease. *Annu*. *Rev*. *Neurosci*. **34**, 185 (2011).
8. Zhang, C. & Saunders, A. J. Therapeutic Targeting of the Alpha-Secretase Pathway to Treat Alzheimer's Disease. *Discov*. *Med*. **7**, 113–117 (2009).
9. Hardy, J. A. & Higgins, G. A. Alzheimer's disease: The amyloid cascade hypothesis. *Science (80-.)*. **256**, 184–185 (1992).
10. Lambert, M. P. *et al*. Diffusible, nonfibrillar ligands derived from Aβ1–42 are

potent central nervous system neurotoxins. *Proc*. *Natl*. *Acad*. *Sci*. **95**, 6448–6453 (1998).

11. Masliah, E., Terry, R. D., Mallory, M., Alford, M. & Hansen, L. A. Diffuse plaques do not accentuate synapse loss in Alzheimer's disease. *Am*. *J*. *Pathol*. **137**, 1293 (1990).

12. Hsia, A. Y. *et al*. Plaque-independent disruption of neural circuits in Alzheimer's disease mouse models. *Proc*. *Natl*. *Acad*. *Sci*. *U*. *S*. *A*. **96**, 3228–3233 (1999).

13. Jucker, M. & Walker, L. C. Pathogenic Protein Seeding in Alzheimer's Disease and Other Neurodegenerative Disorders. *Ann*. *Neurol*. **70**, 532 (2011).

14. Bhopatkar, A. A. & Rangachari, V. Are granulins copper sequestering proteins? *Proteins Struct*. *Funct*. *Bioinforma*. **89**, 450–461 (2021).

15. Konstantoulea, K., Louros, N., Rousseau, F. & Schymkowitz, J. Heterotypic interactions in amyloid function and disease. *FEBS J*. (2021).

16. Davies, P. & Maloney, A. J. F. Selective loss of central cholinergic neurons in Alzheimer's disease. *Lancet (London, England)* **2**, 1403 (1976).

17. Coyle, J. T., Price, D. L. & DeLong, M. R. Alzheimer's disease: a disorder of cortical cholinergic innervation. *Science* **219**, 1184–1190 (1983).

18. Muir, J. L. Acetylcholine, aging, and Alzheimer's disease. *Pharmacol*. *Biochem*. *Behav*. **56**, 687–696 (1997).

19. Dhakal, S., Saha, J., Wyant, C. E. & Rangachari, V. αS oligomers generated from polyunsaturated fatty acid and dopamine metabolite differentially interact with Aβ to enhance neurotoxicity. *bioRxiv* 2021.08.08.455587 (2021) doi:10.1101/2021.08.08.455587.

20. Pettegrew, J. W., Panchalingam, K., Hamilton, R. L. & Mcclure, R. J. Brain membrane phospholipid alterations in Alzheimer's disease. *Neurochem*. *Res*. **26**, 771–782 (2001).

21. Waschuk, S. A., Elton, E. A., Darabie, A. A., Fraser, P. E. & McLaurin, J. A. Cellular Membrane Composition Defines Aβ-Lipid Interactions*. *undefined* **276**, 33561–33568 (2001).

22. Bokvist, M., Lindströ, F., Watts, A. & Grö Bner, G. Two Types of Alzheimer's b-Amyloid (1-40) Peptide Membrane Interactions: Aggregation Preventing Transmembrane Anchoring Versus Accelerated Surface Fibril Formation. doi:10.1016/j.jmb.2003.11.046.

23. Korshavn, K. J., Bhunia, A., Lim, M. H. & Ramamoorthy, A. Amyloid-β adopts a conserved, partially folded structure upon binding to zwitterionic lipid bilayers prior to amyloid formation. *Chem*. *Commun*. *(Camb)*. **52**, 882 (2016).

24. Chauhan, A., Ray, I. & Chauhan, V. P. S. Interaction of amyloid beta-protein with anionic phospholipids: possible involvement of Lys28 and C-terminus aliphatic amino acids. *Neurochem*. *Res*. **25**, 423–429 (2000).

25. Lee, S., Fernandez, E. J. & Good, T. A. Role of aggregation conditions in structure, stability, and toxicity of intermediates in the Aβ fibril formation pathway. *Protein Sci*. **16**, 723 (2007).

26. Good, T. A. & Murphy, R. M. Aggregation State-Dependent Binding of β-Amyloid Peptide to Protein and Lipid Components of Rat Cortical Homogenates. *Biochem*. *Biophys*. *Res*. *Commun*. **207**, 209–215 (1995).

27. Kremer, J. J. & Murphy, R. M. Kinetics of adsorption of β-amyloid peptide Aβ(1–

40) to lipid bilayers. *J*. *Biochem*. *Biophys*. *Methods* **57**, 159–169 (2003).

28. Yamamoto, N., Hasegawa, K., Matsuzaki, K., Naiki, H. & Yanagisawa, K. Environment- and mutation-dependent aggregation behavior of Alzheimer amyloid beta-protein. *J*. *Neurochem*. **90**, 62–69 (2004).

29. Kumar, A., Bullard, R. L., Patel, P., Paslay, L. C. & Singh, D. Non-Esterified Fatty Acids Generate Distinct Low-Molecular Weight Amyloid-b (Ab42) Oligomers along Pathway Different from Fibril Formation. *PLoS One* **6**, 18759 (2011).

30. Kumar, A. *et al*. Specific soluble oligomers of amyloid-β peptide undergo replication and form non-fibrillar aggregates in interfacial environments. *J*. *Biol*. *Chem*. **287**, 21253–21264 (2012).

31. Dean, D. N. *et al*. Strain-specific Fibril Propagation by an Aβ Dodecamer. *Sci*. *Reports 2017 71* **7**, 1–13 (2017).

32. Choo-Smith, L. P. I. & Surewicz, W. K. The interaction between Alzheimer amyloid β(1–40) peptide and ganglioside GM1-containing membranes. *FEBS Lett*. **402**, 95–98 (1997).

33. Yanagisawa, K., Odaka, A., Suzuki, N. & Ihara, Y. GM1 ganglioside–bound amyloid β–protein (Aβ): A possible form of preamyloid in Alzheimer's disease. *Nat*. *Med*. *1995 110* **1**, 1062–1066 (1995).

34. Kakio, A., Nishimoto, S. ichi, Yanagisawa, K., Kozutsumi, Y. & Matsuzaki, K. Interactions of amyloid beta-protein with various gangliosides in raft-like membranes: importance of GM1 ganglioside-bound form as an endogenous seed for Alzheimer amyloid. *Biochemistry* **41**, 7385–7390 (2002).

35. Saha, J. *et al*. Biophysical characteristics of lipid-induced Aβ oligomers correlate

to distinctive phenotypes in transgenic mice. *FASEB J*. **35**, (2021).

36. Yamamoto, N. *et al*. Assembly of hereditary amyloid β-protein variants in the presence of favorable gangliosides. *FEBS Lett*. **579**, 2185–2190 (2005).

37. Laurine, E. *et al*. Lithostathine Quadruple-helical Filaments Form Proteinase K-resistant Deposits in Creutzfeldt-Jakob Disease *. *J*. *Biol*. *Chem*. **278**, 51770–51778 (2003).

38. Piccardo, P. *et al*. Proteinase-K-Resistant Prion Protein Isoforms in Gerstmann-Straussler-Scheinker Disease (Indiana Kindred). *J*. *Neuropathol*. *Exp*. *Neurol*. **55**, 1157–1163 (1996).

39. Bocharova, O. V. *et al*. Annealing prion protein amyloid fibrils at high temperature results in extension of a proteinase K-resistant core. *J*. *Biol*. *Chem*. **281**, 2373–2379 (2006).

40. Murakami, K. *et al*. Synthetic and Biophysical Studies on the Toxic Conformer in Amyloid β with the E22Δ Mutation in Alzheimer Pathology. *ACS Chem*. *Neurosci*. **11**, 3017–3024 (2020).

41. Kracun, I. *et al*. Human brain gangliosides in development, aging and disease. *Int*. *J*. *Dev*. *Biol*. **35**, 289–295 (2002).